Electronic Supplementary Material (ESI) for Journal of Materials Chemistry B.

Multifunctional 3D sponge-like macroporous cryogel-modified long carbon fiber reinforced polyetheretherketone implant with enhanced vascularization and osseointegration

Wenying Dong [1], Wendi Ma [1], Shanshan Zhao [1], Xingyu Zhou [1], Yilong Wang [1], Zhewen Liu [2], Dahui Sun [2], Mei Zhang [1*], Zhenhua Jiang [1]

1. *Key Laboratory of High Performance Plastics, Ministry of Education, College of Chemistry, Jilin University, Changchun 130012, P. R. China;*

2. *Norman Bethune First Hospital, Jilin University, Changchun 130021, P. R. China*

**Corresponding author: zhangmei@jlu.edu.cn*

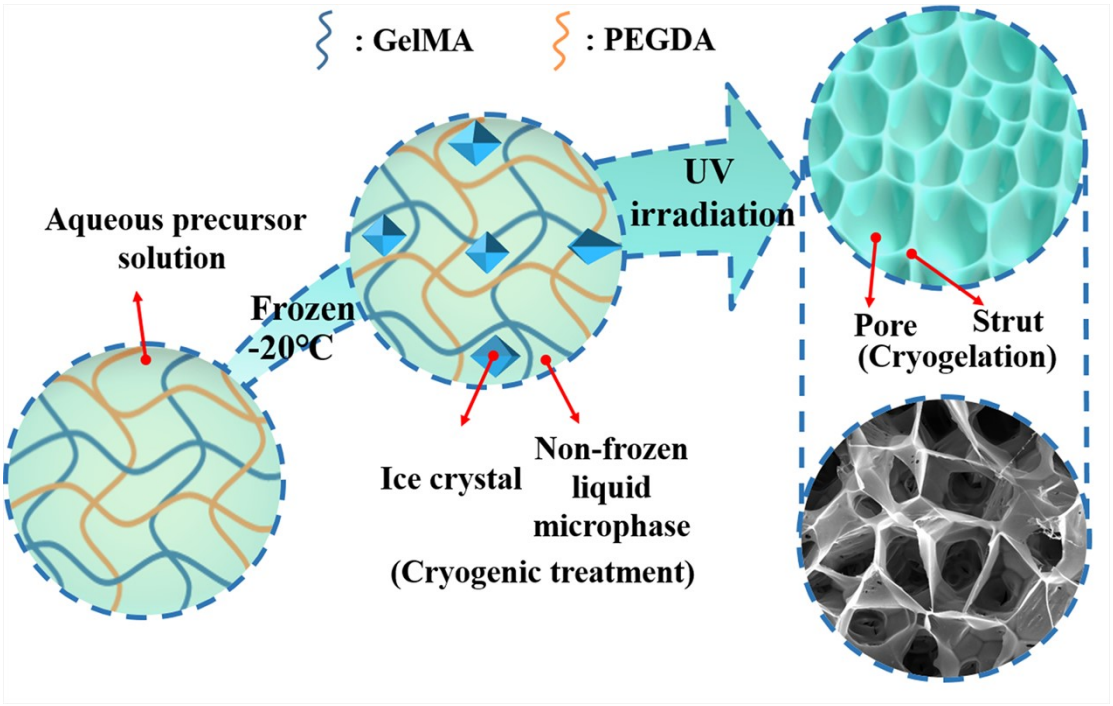

Fig. S1. Schematic depiction of the GelMA/PEGDA cryogel on the surface of the sulfonated LCFRPEEK formation.

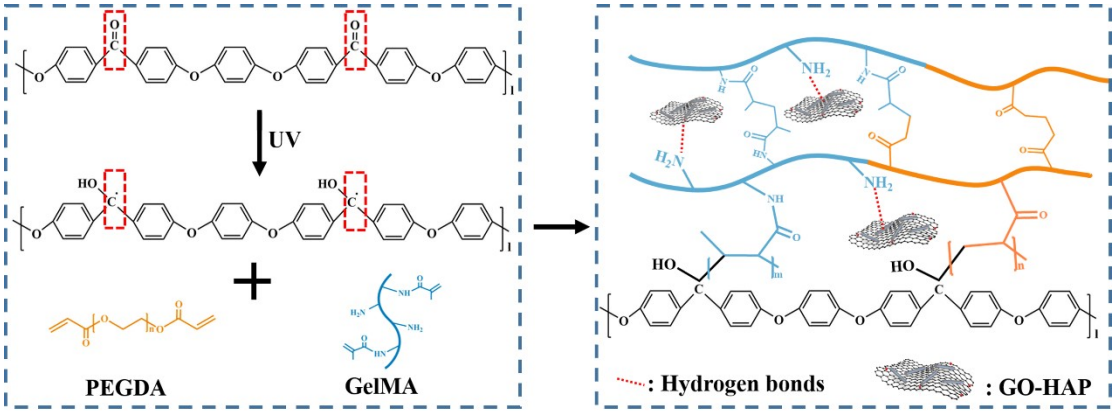

Fig. S2. Schematic illustration of the free radical polymerization on the surface of LCFRPEEK.

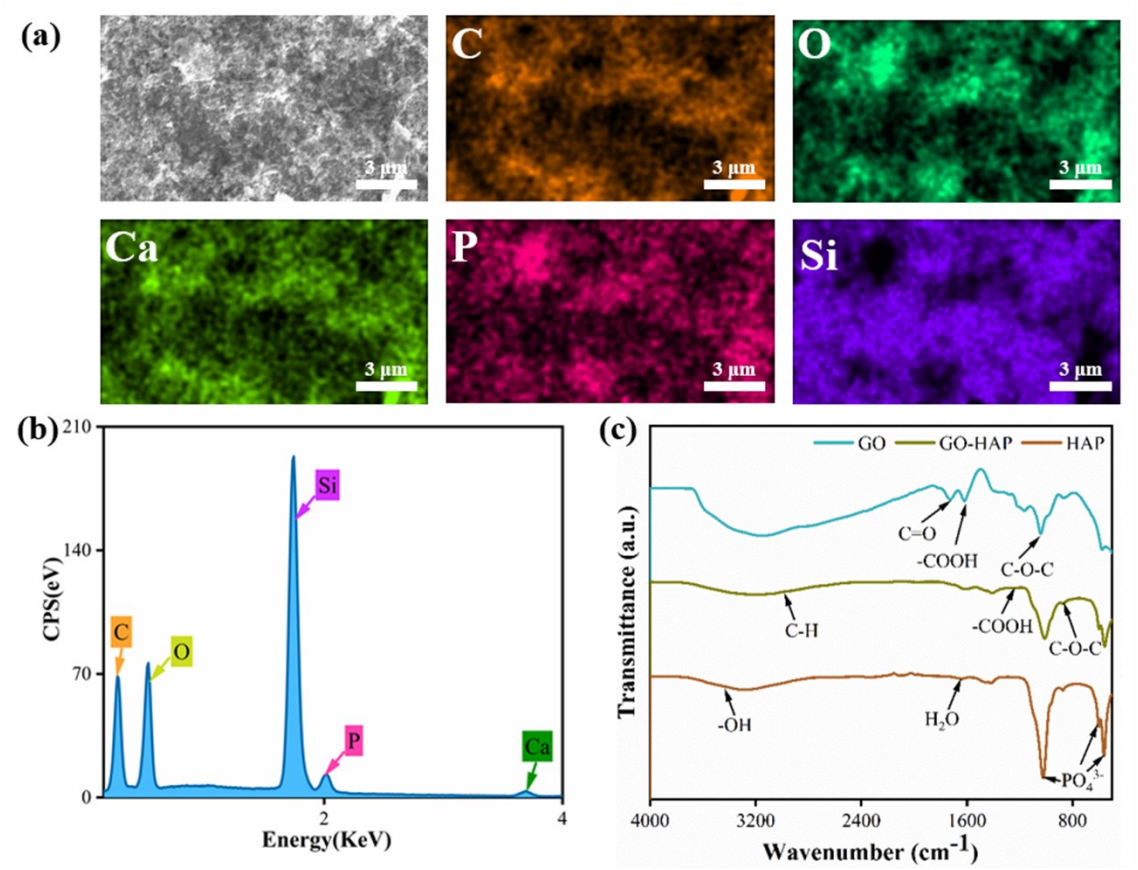

Fig. S3. (a) EDS images and (b) spectra of GO-HAP nanocomposite. (c) ATR-FTIR spectra of GO, HAP, and GO-HAP.

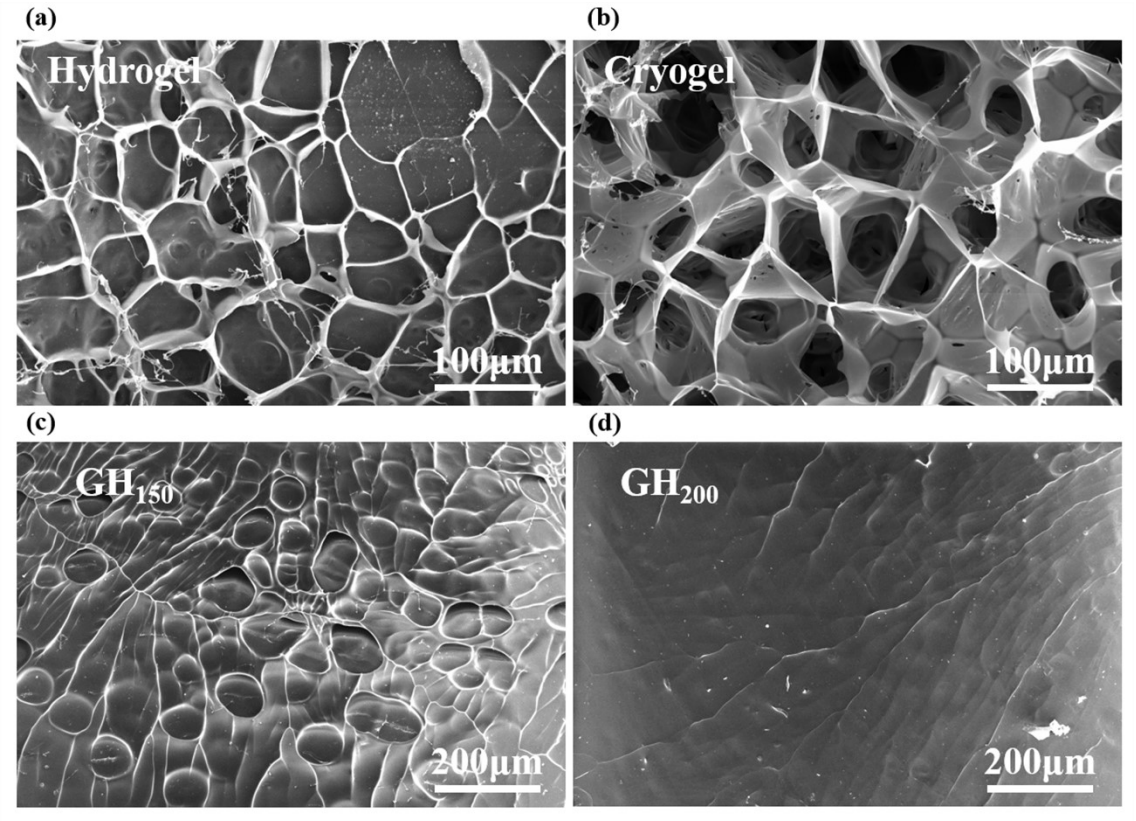

Fig. S4. (a) SEM images of GelMA/PEGDA hydrogel on the surface of sulfonated LCFRPEEK. [GelMA: PEGDA=10:5 wt%, the preparation method of GelMA/PEGDA hydrogel on the surface of sulfonated LCFRPEEK was similar to cryogel whereas without the freezing step.] (b) SEM images of GelMA/PEGDA cryogel on the surface of sulfonated LCFRPEEK. [GelMA: PEGDA=10:5 wt%] (c) SEM images of GH_{150}. [The preparation of GH_{150} was consistent with GH_{100} whereas the concentrations of GO-HAP were 150 ng mL^{-1}.] (d) SEM images of GH_{200}. [The preparation of GH_{200} was consistent with GH_{100} whereas the concentrations of GO-HAP were 200 ng mL^{-1}.]

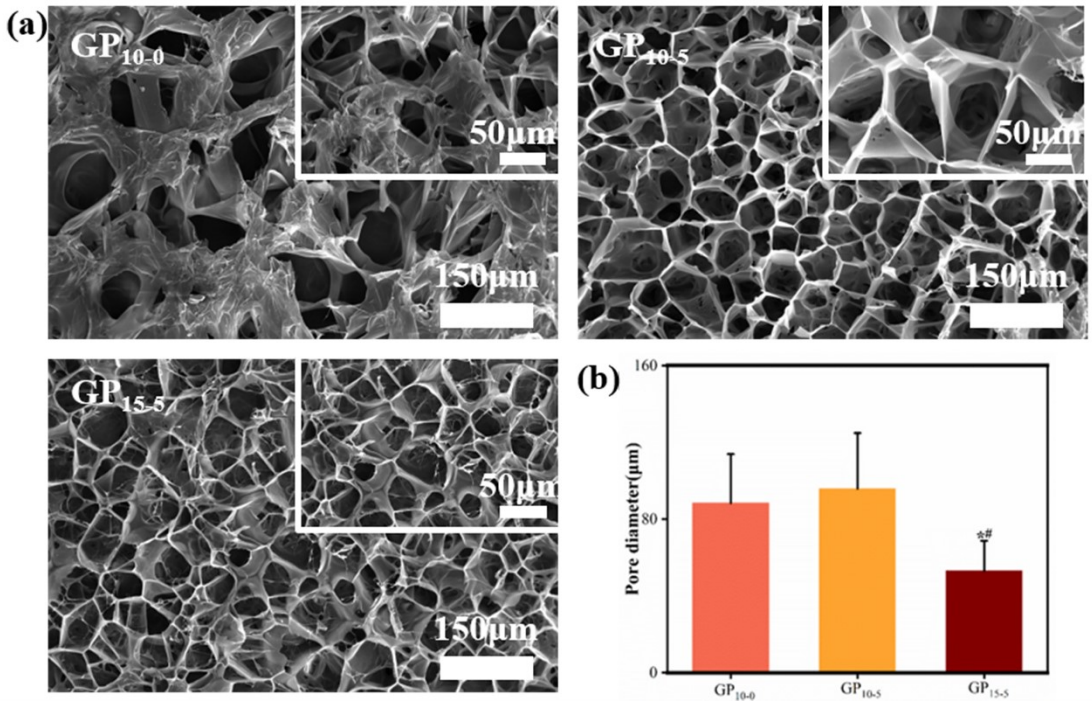

Fig. S5. (a) SEM images of: GP10-0, GP10-5 and GP15-5 at high and low magnifications. Scale bars = 50 μm and 150 μm. (b) The pore diameters of GP10-0, GP10-5 and GP15-5, * and # represented $p < 0.05$ when compared with GP10-0 and GP10-5, respectively.

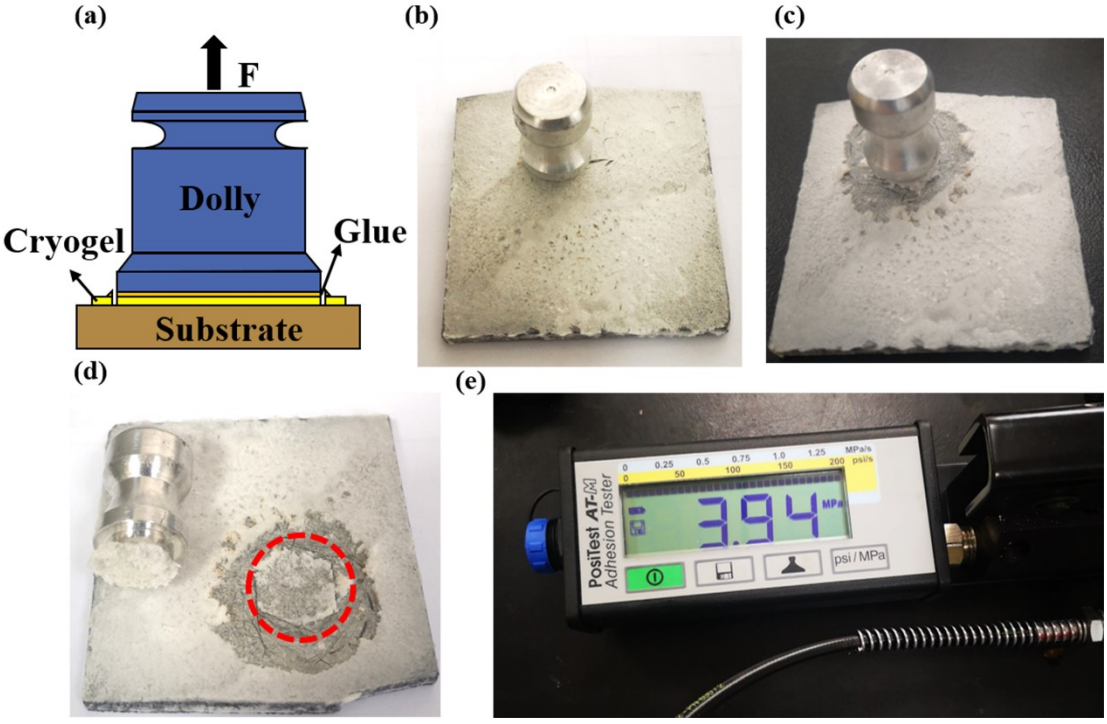

Fig. S6. (a) Diagram of the experimental device of the pull-off method. (b) Image of $GP_{10\text{-}5}$ after adhering the dolly with epoxy glue. (c) Image of $GP_{10\text{-}5}$ after cutting by the cutter. (d) Image of $GP_{10\text{-}5}$ and the dolly after pull-off test. (e) Adhesion data of $GP_{10\text{-}5}$.

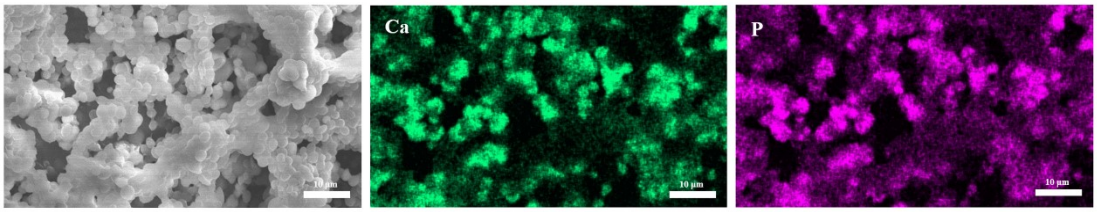

Fig. S7. EDS images of GH_{100} after soaking in SBF for 7 days. Scale bars = 10 μm.

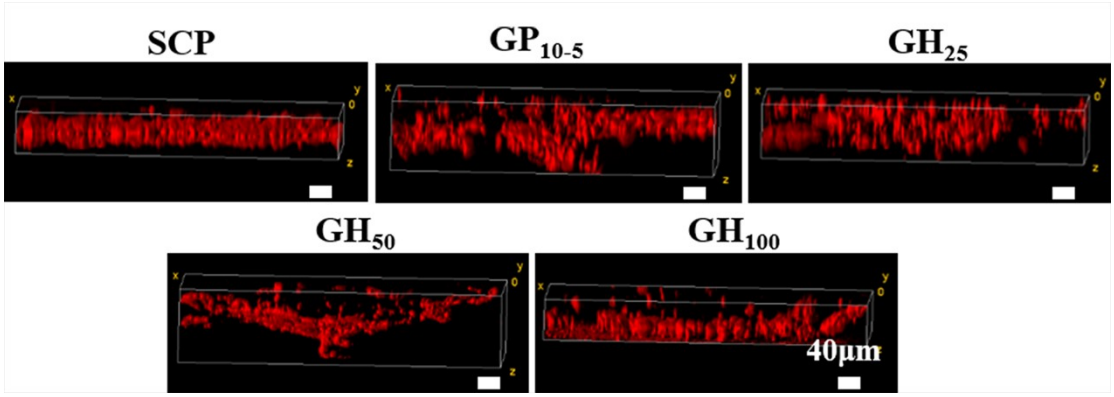

Fig. S8. Representative 3D CLSM images of HUVEC migration into different scaffolds stained using TRITC-phalloidin for cytoskeletal organization. Scale bars = 40 μm.

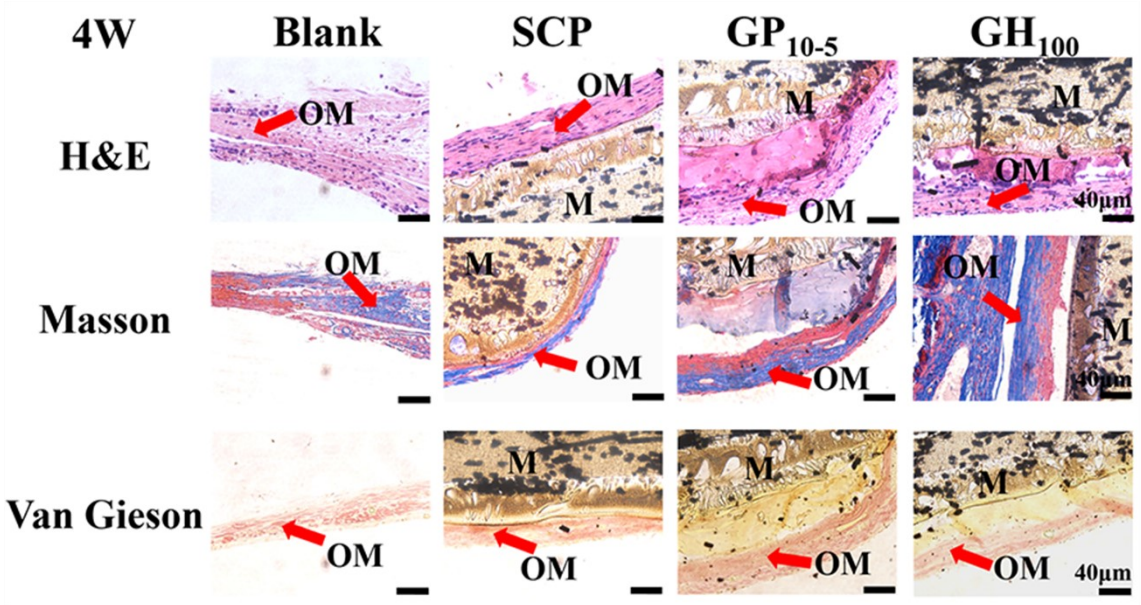

Fig. S9. H & E, Masson and Van Gieson staining of the calvarial defect regions after treatment with different samples for 4 weeks. Scale bars = 40 μm. [M, Materials; OM, osteoid matrix (red arrows)].

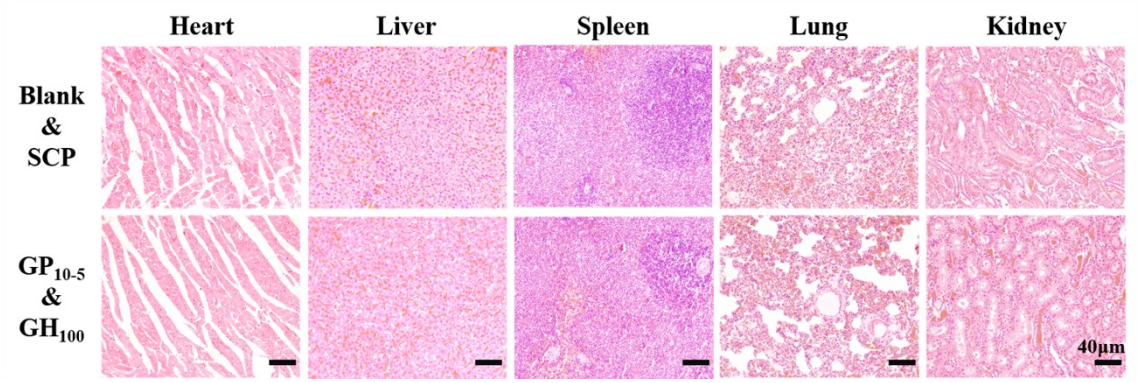

Fig. S10. Histological observation of H & E staining of tissues (heart, liver, spleen, lung, and kidney) after 12 weeks of treatments. Scale bar = 40 μm.

Table S1 Primer pairs used in RT-PCR analysis.

Genes	Forward primer sequence (5′-3′)	Reverse primer sequence (5′-3′)
BMP-2	ATTAGCAGGTCTTTGCACCA	ACGCTTTTCTCGTTTGTGGA
Runx2	GGCAGCACGCTATTAAATCCA A	GACTCATCCATTCTGCCGCTA
ALP	ATCGGAACAACCTGACTGACC	CTGCCTCCTTCCACTAGCAA
COL-I	ATGCCATCAAGGTCTACTGCAA	GAACCTTCGCTTCCATACTCG
GAPDH	TATGACTCTACCCACGGCAAG	ATACTCAGCACCAGCATCACC

Table S2 Elemental composition of different substrate surfaces as determined by XPS.

Material	C (%)	N (%)	O (%)	S (%)	Ca (%)	P (%)
SCP	58.84	---	40.06	1.09	---	---
$GP_{10\text{-}5}$	41.17	10.11	48.72	---	---	---
GH_{100}	44	12.46	40.97	---	1.6	0.96

Table S3 Changes in Ca and P content of GH_{100} sample before and after immersion in SBF by EDS.

Sample	Ca (%)	P (%)	Ca/P
Before immersion in SBF	1.6	0.96	1.67
After immersion in SBF	3.87	2.1	1.84
New bone-like apatite	2.27	1.14	1.99